iScience, Volume *23*

Supplemental Information

Multiscale ATUM-FIB Microscopy Enables Targeted Ultrastructural Analysis at Isotropic Resolution

Georg Kislinger, Helmut Gnägi, Martin Kerschensteiner, Mikael Simons, Thomas Misgeld, and Martina Schifferer

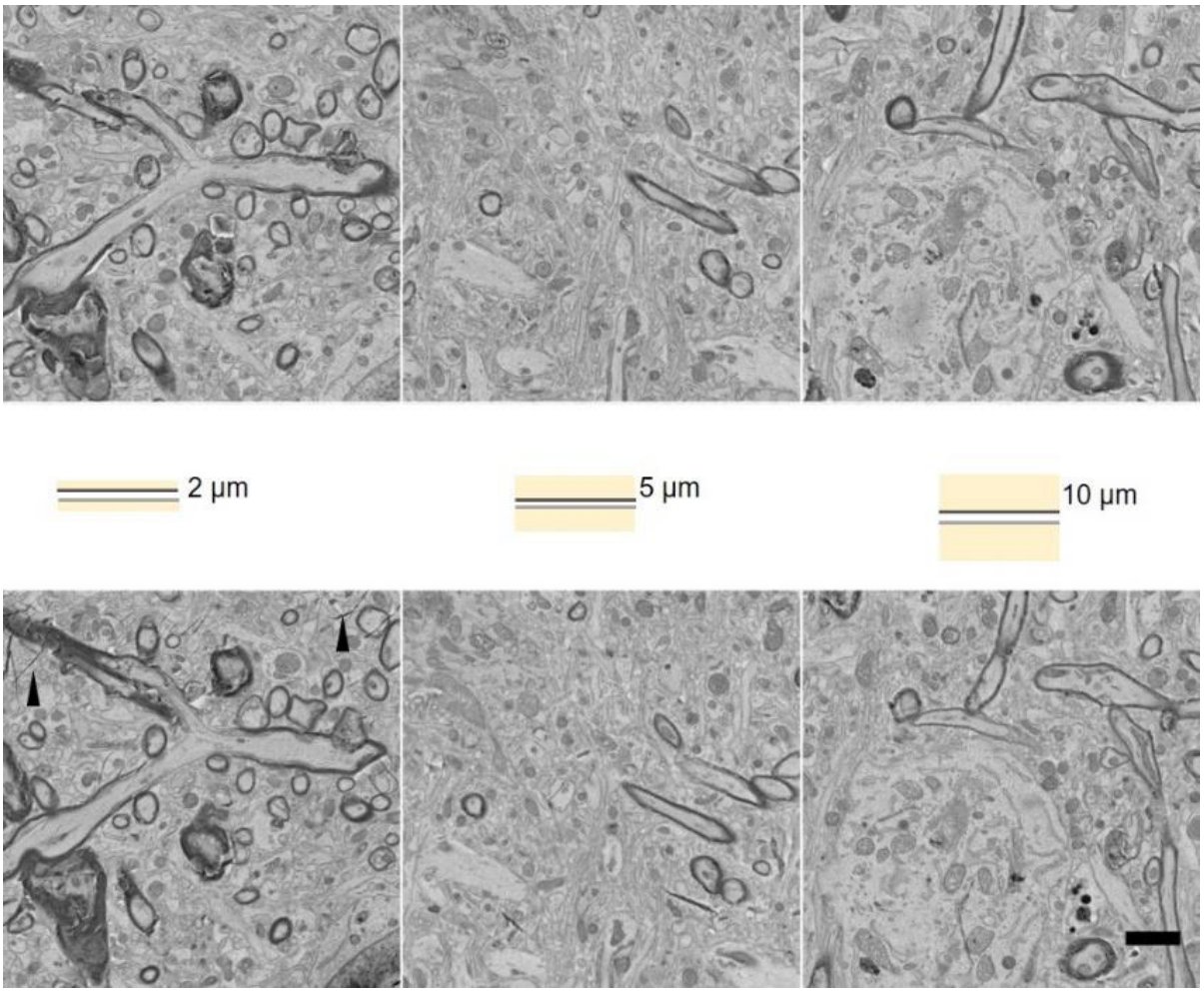

Figure S1. Consecutive semithick section tissue loss. Related to Figure 2. Middle panel shows schematics of opposing section surfaces revealing one section top face (light grey) and the bottom side of the consecutive one (dark grey). The remaining cross section thickness is shown in yellow. Top and bottom panels show matching BSD images of consecutive 2, 5 and 10 µm sections. The first row shows the bottom of one section and the lower row shows the opposing surface of the following section. The latter were turned upside down and deposited on CNT tape. Folds (arrowhead) could not be prevented in this turning procedure of thinner sections (< 5 µm). Scale bar 2 µm.

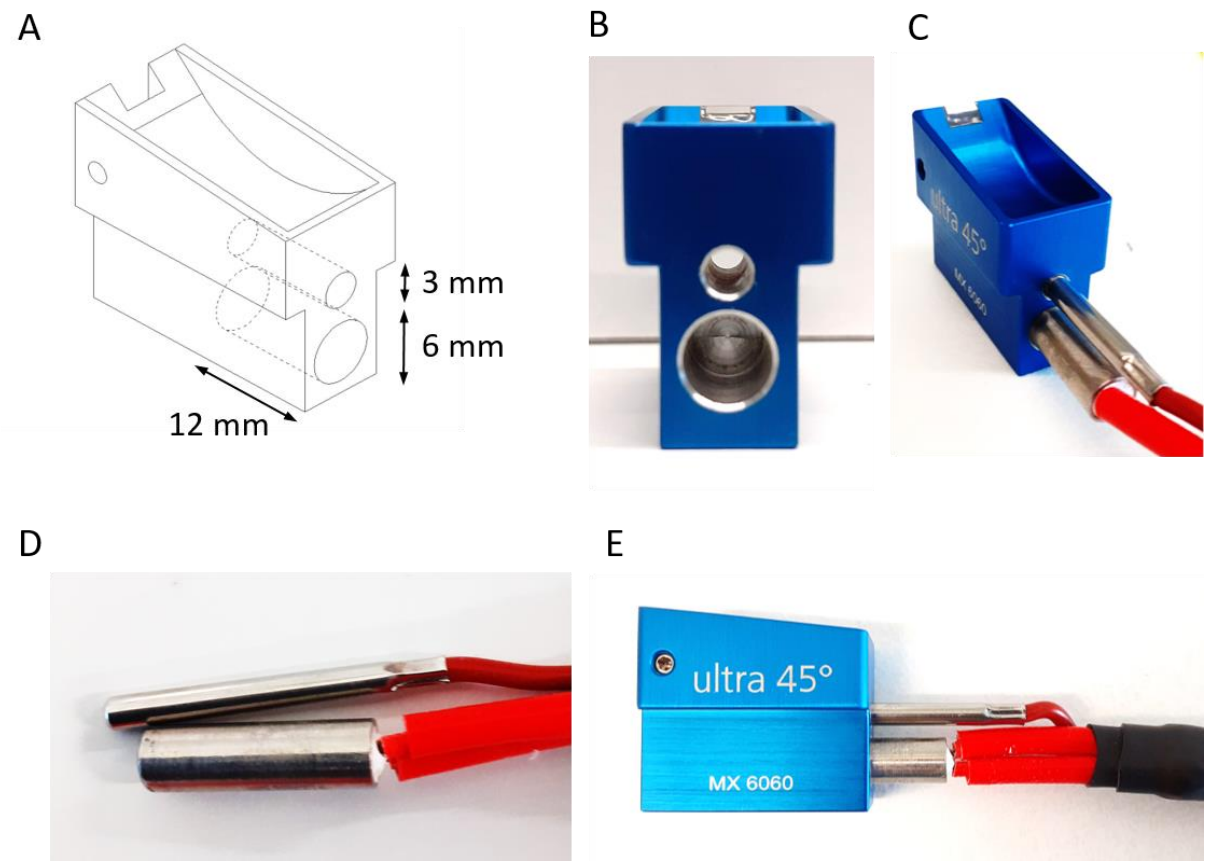

Figure S2. Design details of the heated knife. Related to Figure 3. Construction scheme (A) and photo (B) of the knife tub including the 3 and 6 mm drillings for the sensor and heater elements, respectively. Photographs of the front (C) and side (E) views of the knife boat including upper sensor and lower heater elements (D).

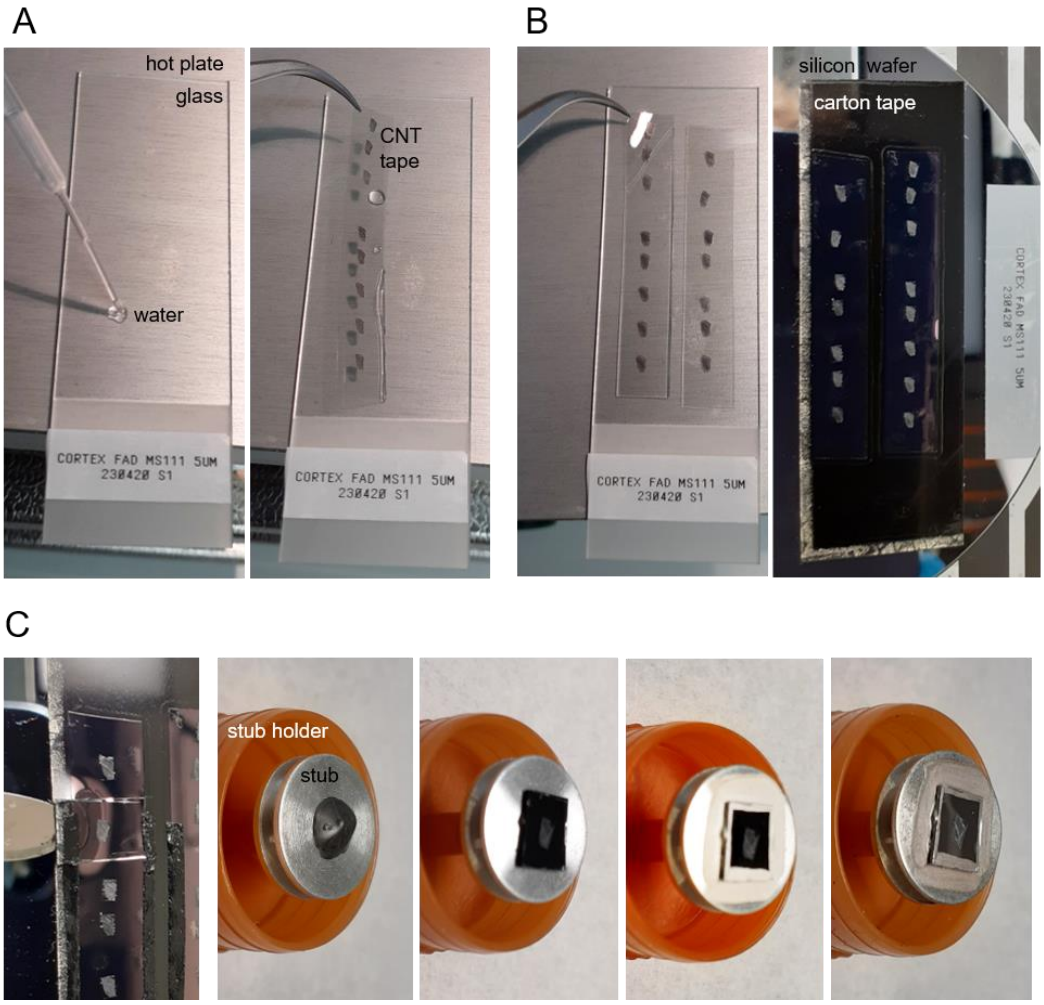

Figure S3. Experimental workflow for section mounting. Related to Figure 3. (A-C) Photos of the mounting steps are shown. (A) For slide scanner imaging a drop of water is placed on the glass slide (left). After the water spreads below the strip of CNT tape with the semithick sections (right), the glass slide is heated on a hot plate (at 60°C) for a few minutes. (B) After light microscopy, the CNT tape strip can be easily removed from the glass slide using a forceps (left). A strip of carbon adhesive tape is placed on a 4 inch silicon wafer and the CNT tape strip attached onto the tape (right). When sections are covered by a piece of plastic, a roller can be used to flatten the tape. (C) Narrow stripes of carbon adhesive tape can be attached between wafer and CNT tape for better grounding (left). Using a scalpel, the section of interest including CNT and carbon adhesive tape is excised from the wafer (left). Carbon adhesive is added on a FIB stub fixed in a stub holder (second) and the piece of section adhered onto it (third). Silver paint is distributed around the tape for better grounding (fourth) and a layer of carbon sputtered on over the surface (right).

Transparent Methods

Animals

For this study we worked with fixed brain tissue of wildtype mice (18 months) and a model expressing five familial AD gene mutations (5xFAD[31]; 2 months) (Oakley et al., 2006). Mice were group-housed under pathogen-free conditions and bred in the animal housing facility of the Center of Stroke and Dementia Research. All experiments were carried out in compliance with the National Guidelines for Animal Protection, Germany, with the approval of the regional Animal care committee of the Government of Upper Bavaria, and were overseen by a veterinarian.

Sample preparation

Mice were perfused with fixative containing 2.5% glutaraldehyde (Science Services), 2% PFA (Science Services) and 2 mM $CaCl_2$ in 0.1 M sodium cacodylate buffer (Science Services). Brains were dissected and transferred into fixative for incubation at 4°C for two additional days. Tissue sections of maximal 1 mm thickness comprising cortex and corpus callosum regions were prepared.

Fixed samples were stained *en bloc* by a varied rOTO protocol (Tapia et al., 2012, Hua et al., 2015) without lead aspartate. Both, microwave-based (BioWave Pro, Pelco) and bench protocols were successfully applied as detailed in Table 1. We applied a sequence of reduced 2% osmium tetroxide in 0.1 M cacodylate buffer pH 7.4 followed by 2.5% potassium hexacyanoferrate in the same buffer. After washes the tissue was incubated in 1% aqueous thiocarbohydrazide (TCH) and subsequently in 2% aqueous osmium tetroxide. After overnight incubation in 1% uranylacetate at 4°C and 2h in 50°C, samples were dehydrated and infiltrated at least 2h at different resin in acetone concentrations (25, 50, 75, 90%) and overnight and for another 4h in 100% of the respective resin. Durcupan (Science Services) resin was prepared by mixing 11.4 g of component A (epoxy resin), 10.0 g of component B (964 hardener), 0.1 mL of component D (dibutyl phthalate) and component C (964 accelerator). For standard epon (Serva) 21.4 g glycidether 100 with 14.4 g dodecenylsuccinic anhydride (DDSA) and 11.3 g nadic methyl anhydride (NMA) were combined for 10 min and 0.84 mL 2,4,6 tris(dimethylaminomethyl)phenol (DMP-30) were added while stirring for another 20 min. LX112 resin (Ladd Research Industries) (Ellis, 2014) was prepared by mixing 4.5 g of mix A (mixture of 5 g of LX112 and 6,45 g of nonenyl succinic anhydride), 10.5 g

of mix B (mixture of 5 g of LX112 and 4.35 g of NMA) and 0.6 ml of DMP-30 (all components from Ladd Research Industries). Resins were cured at 60 °C for 10 or 48 h. Curing times below 10 h did not result in properly hardened blocks.

Automated tape-collecting ultramicrotomy (ATUM)

Epon blocks were roughly trimmed with EM TRIM2 (Leica) and subsequently, a rectangular tissue block (~ 2 x 1.5 x 0.2-0.4 µm) was exposed using the trimtool 45 diamond knife (Diatome). Thick sections were initially generated using a histo jumbo knife (45°, 6 mm, Diatome) in a RMC ultramicrotome (Powertome). The 35° and 45° ultra knife boats for the custom-made heated knives were provided by Diatome. Two holes (3 and 6 mm diameter, respectively) were milled into the base part of the knife boat to fit a temperature sensor (cable probe 3 x 30 mm, Sensorshop24) and a heater (Hotend Heater Catridge CNC for 3D printer, 24V, 40W; Ebay). We used a digital on/off temperature regulator (for PT100, Sensorhop24). Standard infrared lights (230 V, 150 W, Conrad Electronics) were installed at both sides of the microtome. Temperature was controlled by standard probe (VWR) and infrared thermometers (Conrad Electronics) to values within the range of 35-45 °C.

Single sections were fished from the water bath by ~0.3 x 0.8 mm carbon nanotube tape (CNT) tape (Science Services) pieces using inverse forceps. For serial sectioning the RMC tape collector was adapted to the knife by bypassing the tension lever and guiding the CNT tape behind the knife directly to the collector nose. Sectioning speed was set to 0.2-0.3 mm/sec with increased tape speed within (0.4 mm/sec) and reduced tape speed outside (0.1 mm/sec) the cutting window. This assured efficient uptake and minimization of empty intersection space on the tape. Slow speed was required both for limiting compression, as well as for keeping the sections longer in the heated water bath to smoothen. If needed, sections were guided onto the tape collector using fine brushes.

Slide scanner serial light microscopy

For light microscopic investigation, CNT tape strips with single sections or 5 cm strips with serial sections were positioned on a glass slide. For better adherence, a few drops of water were placed between tape and glass and the slide put onto a heating plate at 60 °C (see Figure S3A). Good adherence was important for tape flattening as a prerequisite of the slide scanner autofocusing function. Serial transmitted light

microscopy was performed on a slide scanner (Pannoramic MIDI II 2.0.5, 3D Histech). We selected sections by thresholding and imaged using the autofocusing and the extended focus level functions (9 focus levels, focus step size 0.2 µm x 5) using the 20x objectives. By choosing the extended focus option, the software selects the sharpest image from each focus level for each image field, and combines them into one single image. The autofocus was restricted and the range set by testing it for several sections on different slide locations. Jpeg files were generated from the original data using the Pannoramic software CaseViewer2.2 (3D Histech).

Serial scanning electron microscopy

Sections on glass slides were postcured for 30-48 h at 60 °C. CNT strips with tissue sections were detached and assembled onto carbon tape (Science Services), mounted onto a 4-inch silicon wafer (Siegert Wafer) and grounded with adhesive carbon tape (see Figure S3B). Serial section images were acquired on a Crossbeam Gemini 340 SEM (Zeiss) in backscatter mode at 4 keV (high gain) at 7-8 mm WD and 30 or 60 µm aperture. In ATLAS5 Array Tomography (Fibics, Ottawa, Canada) a wafer overview map at 1000-3000 nm/pixel was generated. On this basis, sections were mapped and imaged at medium (60 x 60 – 100 x 100 nm) resolution. Regions of interest from these section sets were acquired at 10x10 nm/pixel (2 µs dwell time, line average 2). Image series were aligned in TrakEM2 using a combination of automated and manual steps, registered and analysed in Fiji (Schindelin et al., 2012).

Focused Ion Beam Scanning Electron Microscopy (FIB-SEM)

Selected thick sections on CNT tape were cut from the silicon wafer including the adhesive carbon tape underneath using a scalpel (see Figure S3C). Theses samples were mounted with conductive carbon cement (LEIT-C, Plano) and conductive silver colloid (Plano) onto standard aluminum specimen mount (Science Services). A thin layer of carbon was sputtered onto the sections (carbon cord, Science Services; sputter coater Q150T ES, Quorum). Milling and imaging were performed on a Crossbeam Gemini 340 FIB-SEM operating under SmartSEM (Zeiss) and Atlas-3D (Fibics Incorporated). Ion beam currents of 50 pA - 15 nA were used. The milling rate was set to 5 nm slices. SEM images were recorded with an aperture of 60 µm in the high current mode at 2 kV of the InlenseDuo detector with the BSE grid set to 300-500 V and the SE detector. Voxel sizes of 5 x 5 x 5 nm were chosen. Images series of

1000-2000 consecutive sections were recorded. In ATLAS, the milling current and depth were adjusted to match with exposure time of the SEM (line average 2, dwell time 3 µs). Automatic correction of focus (auto tune) and astigmatism (auto stig) was applied every 30 minutes. FIB-SEM image stacks were aligned and analyzed in Fiji (Schindelin et al., 2012). VAST (Berger et al., 2018) was used for segmentation and Blender for rendering of the 3D models (Community, 2017).

Key Resource Table

REAGENT or RESOURCE	SOURCE	IDENTIFIER
Chemicals and Materials		
Cable sensor	SensorShop24	Cat# 003-KS-PT100-2L-1.0-330-W
Carbon adhesive tape	Science Services	Cat# P77819-25
Controller for PT100	SensorShop24	Cat# TR-PT100-A-24V
Diamond knife 35°, 45°, 3 mm	Diatome	Cat# DU3530; DU4530,
Epon (Glycid ether 100, MNA, DDSA, DMP-30)	Serva	Cat# 21045.02, 29452.05, 20755.02, 36975.01,
Glutaraldehyde	Science Services	Cat# E16216
Heating cartridge, 24V, 40W	Ebay	N/A
Leit-C	Plano	Cat# G3300
Leitsilber, Acheson 1415	Plano	Cat# G3692
LX112 Embedding Kit	LADD Research Laboratories	Cat# 21210
Osmium tetroxide	Science Services	Cat# E19130
Paraformaldehyde	Science Services	Cat# E15713

Potassium hexacyanoferrate(II) trihydrate	Sigma	Cat# 455989
Silicon wafer, 4'', 1-side polished, p-type (Boron), 1-0 Ohm cm	MicroChemicals	Cat# WSM40525200P1334SNN1
Sodium cacodylate trihydrate	Science Services	Cat# E12300
Specimen mount	Science Services	Cat# 7536-30
Thiocarbohydrazide	Sigma-Aldrich	Cat# 223220
Uranyl acetate	Science Services	Cat# E22400-05G
Experimental Models: Organisms/Strains		
wt mice	The Jackson Laboratory	C57BL/6J
5xFAD[31] (five human familial AD gene mutations) mice	MMRRC	Stock# 34840-JAX / 5XFAD
Software and Algorithms		
ImageJ 2.0.0	NIH	https://imagej.nih.gov/ij/; RRID:SCR_003070
VAST	Harvard	https://software.rc.fas.harvard.edu/lichtman/vast/
Blender	The Blender Foundation	https://www.blender.org/
SmartSEM	Carl Zeiss Microscopy GmbH	N/A
ATLAS 5, Array Tomography, 3D	Fibics Incorporated, Canada	N/A

Berger, D. R., Seung, H. S. and Lichtman, J. W. (2018) 'VAST (Volume Annotation and Segmentation Tool): Efficient Manual and Semi-Automatic Labeling of Large 3D Image Stacks', *Frontiers in Neural Circuits,* 12, pp. 88.

Community, B. O. 2017. Blender-a 3D modelling and rendering package. Blender Foundation, Blender Institute Amsterdam.

Ellis, E. A. (2014) 'No More Epon 812: This Product Does Not Exist Today', *Microscopy Today,* 22(3), pp. 50-53.

Hua, Y., Laserstein, P. and Helmstaedter, M. (2015) 'Large-volume en-bloc staining for electron microscopy-based connectomics', *Nature Communications,* 6, pp. 7923.

Oakley, H., Cole, S. L., Logan, S., Maus, E., Shao, P., Craft, J., Guillozet-Bongaarts, A., Ohno, M., Disterhoft, J., Van Eldik, L., Berry, R. and Vassar, R. (2006) 'Intraneuronal beta-amyloid aggregates, neurodegeneration, and neuron loss in transgenic mice with five familial Alzheimer's disease mutations: potential factors in amyloid plaque formation', *J Neurosci,* 26(40), pp. 10129-40.

Schindelin, J., Arganda-Carreras, I., Frise, E., Kaynig, V., Longair, M., Pietzsch, T., Preibisch, S., Rueden, C., Saalfeld, S., Schmid, B., Tinevez, J. Y., White, D. J., Hartenstein, V., Eliceiri, K., Tomancak, P. and Cardona, A. (2012) 'Fiji: an open-source platform for biological-image analysis', *Nat Methods,* 9(7), pp. 676-82.

Tapia, J. C., Kasthuri, N., Hayworth, K. J., Schalek, R., Lichtman, J. W., Smith, S. J. and Buchanan, J. (2012) 'High-contrast en bloc staining of neuronal tissue for field emission scanning electron microscopy', *Nat Protoc,* 7(2), pp. 193-206.